

- South Windsor, CT, Rep. No. DOE/NASA/0191-1 (1984).
6. T. Sira and M. Ostensad, in *Solid Oxide Fuel Cells*, S. C. Singhal and H. Iwahara, Editors, PV 93-4, p. 851, The Electrochemical Society Proceedings Series, Pennington, NJ (1993).
 7. M. Dokiya, N. Sakai, T. Kawada, and H. Yokokawa, in *Proceedings of the International Fuel Cell Conference*, p. 309, Makuhari, Japan (1992).
 8. R. A. Gaggioli and W. R. Dunbar, *Trans. ASME*, **115**, 100 (1993).
 9. A. Solheim, R. Tunold, and R. Ødegard, in *Solid Oxide Fuel Cells*, F. Gross, P. Zegers, S. C. Singhal, and O. Yamamoto, Editors, p. 297, Commission of the European Communities, Luxembourg (1991).
 10. D. G. Walhood and J. R. Ferguson, *ibid.*, p. 289.
 11. J. Hartvigsen, S. Elangovan, and A. Khandkar, in *Solid Oxide Fuel Cells*, S. C. Singhal and H. Iwahara, Editors, PV 93-4, p. 878, The Electrochemical Society Proceedings Series, Pennington, NJ (1993).
 12. I. V. Yentekakis, S. Neophytides, S. Seimanides, and C. G. Vayenas, in *Solid Oxide Fuel Cells*, F. Gross, P. Zegers, S. C. Singhal, and O. Yamamoto, Editors, p. 281, Commission of the European Communities, Luxembourg (1991).
 13. E. Erdle, J. Gross, H. G. Müller, W. J. C. Müller, H. -J. Reusch, and R. Sonnenschein, *ibid.*, p. 265.
 14. J. R. Ferguson, *ibid.*, p. 305.
 15. J. Hartvigsen, S. Elangovan, and A. Khandkar, in *Science and Technology of Zirconia V*, S. P. S. Badwal, M. J. Bannister, R. H. J. Hannink, Editors, p. 682, Technomic Publishing Company Inc., Lancaster, PA (1993).

Electrolyte Effects on Spinel Dissolution and Cathodic Capacity Losses in 4 V Li/Li_xMn₂O₄ Rechargeable Cells

Dong H. Jang and Seung M. Oh*

Department of Chemical Technology, College of Engineering, Seoul National University, Seoul 151-742, Korea

ABSTRACT

Spinel dissolution and cathodic capacity losses in 4 V Li/Li_xMn₂O₄ secondary cells were examined in various electrolyte solutions comprising different solvents and Li salts. It was found that spinel dissolution is induced by acids that are generated as a result of electrochemical oxidation of solvent molecules on composite cathodes. Among various organic solvents, ethers such as tetrahydrofuran and dimethoxyethane were readily oxidized to produce acids whereas carbonates (ethylene carbonate, propylene carbonate, diethylcarbonate) were relatively inert. Consequently, when a spinel-loaded composite cathode was charge/discharge cycled in the potential range of 3.6 to 4.3 V (*vs.* Li/Li⁺), both the acid concentration and the extent of spinel dissolution was much higher in the ether-containing electrolytes as compared to the carbonates. The results, obtained from the chemical analysis on acid-attacked spinel powders and from the open-circuit potential measurement of composite cathodes, indicated that Li and Mn ion extraction is dominant in the earlier stage of acid attack. As the spinel dissolution further continues, however, oxygen losses from the lattice become more important. The combined feature of solvent oxidation and spinel dissolution was also affected by the nature of lithium salts added. Generally, the solvent-derived acid generation was not significant in those electrolytes containing fluorinated salts (LiPF₆, LiBF₄, and LiAsF₆), yet the spinel dissolution in these electrolytes was still appreciable because acids were generated via another pathway; a reaction between the F-containing anions and impurity water.

Introduction

Spinel manganese oxides are among the promising cathode materials for lithium secondary batteries.¹⁻¹³ When Li_xMn₂O₄ cathodes are cycled in the 4 V range ($x = 0.0$ to 1.0), their cyclability is generally better than 3 V cells ($x = 1.0$ to 2.0).¹¹⁻¹³ The poor cyclability in the latter cells is known to be caused by Jahn-Teller distortion which evolves when the average Mn valence becomes less than 3.5.⁹⁻¹³ Even though the Jahn-Teller distortion is not prevalent in 4 V cells since the average Mn valence is maintained higher than 3.5, many 4 V Li_xMn₂O₄ cathodes still show a slow capacity fade when they are repeatedly cycled.¹¹⁻¹³

Several failure mechanisms of 4 V Li_xMn₂O₄ cathodes have been proposed in the literatures. Dahn *et al.*¹⁴ interpreted the failure in terms of oxygen losses from the spinel lattice which were suggested to be caused by the reaction with electrolyte. Specifically, they provided evidence, *viz.*, the discharge plateau which appeared at 3.3 V, for the formation of oxygen-deficient spinels. Tarascon *et al.*¹⁵ accounted for the capacity losses with a cation mixing between the Li and Mn sites in the spinel lattice. Based on this, they recommended a slow cooling of reaction mixtures to minimize the cation mixing. As another highly plausible explanation, the presence of impurity phases was ascribed by Manev *et al.*,¹⁶ by whom a carefully controlled multistep solid-state reaction was suggested for the preparation of pure spinel oxides.

* Electrochemical Society Active Member.

In a previous paper, we have proposed another failure mode that was derived from a study on the cathodic performances of Li/PC + DME/Li_xMn₂O₄ cells, where PC is propylene carbonate and DME is dimethoxyethane.⁷ There, we demonstrated that appreciable amounts of manganese ions are dissolved from the spinel framework during charge/discharge cycling in the potential range of 3.6 to 4.3 V (*vs.* Li/Li⁺). Spinel dissolution takes place mainly at a charged state (at >4.1 V *vs.* Li/Li⁺) of the composite cathodes, in which potential range an electrochemical oxidation of solvent molecules is also prominent. From this and another observation whereby spinels were dissolved at a faster rate as the carbon loading increased, it was proposed that at the charged state of cathodes, solvent molecules are electrochemically oxidized on the carbon surface and as-generated species promote spinel dissolution. Results of an ac impedance study also revealed that spinel dissolution leads to an increase in contact resistances at the spinel/carbon interface, and also in the electrode reaction resistances for Li⁺ intercalation/deintercalation. A summary of these results led to the conclusion that spinel dissolution induces capacity losses in two different ways; material loss from the loaded spinel and polarization loss due to a cell resistance increment. In that report, however, details on the nature of the active species that is suspected to be generated after the solvent oxidation, and thereby responsible for the spinel dissolution, remain unidentified. Also, neither the spinel dissolution mechanism nor any electrolyte effects (other than PC + DME, LiClO₄) on the extent of solvent oxidation, spinel dissolution, and

cathodic capacity losses were provided. This article deals with these issues.

In this study, in order to gain insight into these problems, the electrochemical oxidation behavior of various electrolyte solutions comprising different organic solvents and lithium salts was investigated. The results show that electrochemical solvent oxidation produces a significant amount of protons and spinels are dissolved by the action of as-generated protons. It also shows that the extent of solvent oxidation is remarkably varied by the nature of solvent itself and also the lithium salts added. These electrolyte-dependent characteristics of solvent oxidation and acid generation is explained based on the redox properties of organic solvents and also by the salt-mediated solvent oxidation. In addition, the way that spinel dissolution proceeds by the action of protons was traced by analyzing their chemical compositions and the open-circuit potentials of spinel electrodes. From this, the effects which spinel dissolution has on the charge/discharge characteristics of composite cathodes were clarified. Finally, the role that impurity water plays in acid generation was identified.

Experimental

Materials.—Powders of spinel manganese oxides were prepared by the citrate gel method as reported earlier.^{7,17,18} To prepare the composite cathodes, spinel powders (surface area = $21.2 \text{ m}^2 \text{ g}^{-1}$) were mixed with Ketjenblack EC and Teflon binder with a weight ratio of 72:20:8. The mixtures were then dispersed in isopropyl alcohol and spread onto a piece of stainless steel Exmet (long dimension = 2 mm, short dimension = 1 mm, apparent area = 1 cm^2), followed by pressing and drying at 120°C for 12 h. The Li contents in spinel powders were analyzed by the ICP (inductively coupled plasma) technique and the Mn contents by the potentiometric titration method as described in the literature.^{19,20} The average Mn valence was then calculated from the chemical analysis data.

Propylene carbonate (PC), ethylene carbonate (EC), diethylcarbonate (DEC), 1,2-dimethoxyethane (DME) were purchased from Ferro Company. They were of electrolyte grade contaminated with $<20 \text{ ppm H}_2\text{O}$. THF (Mitsubishi Company, battery grade, $<20 \text{ ppm H}_2\text{O}$) was used as received. LiBF_4 , LiClO_4 , LiAsF_6 (Tomiyama Company, Limited, lithium battery grade), and LiPF_6 (Hashimoto Company) were used as received. LiCF_3SO_3 (Aldrich Co., 97%) was dried under vacuum at 120°C for 24 h before use.

Cell performance was tested in a beaker-type three-electrode cell, wherein Li foil (Cyprus Company) was used as the anode and reference electrode. In order for the $\text{Li/Li}_x\text{Mn}_2\text{O}_4$ cells to be cathode-limited such that the observed capacity values represented those of spinels, a smaller amount of spinels relative to the Li anode was loaded in the composite cathodes. Normally, 13 mg of spinel powder ($7.2 \times 10^{-5} \text{ eq}$) was loaded in the composite cathodes while 100 mg of Li foil ($1.4 \times 10^{-2} \text{ eq}$) was used as the anode.

Instrumentation.—The charge-discharge profiles were recorded in a beaker-type cell with a home-made instrument. The cutoff voltages for the charge and discharge limits were fixed at 4.3 and 3.6 V (*vs.* Li/Li^+), respectively. Charge/discharge cycling was performed galvanostatically with a current density of 1 mA cm^{-2} . Dissolved Mn^{2+} ions in electrolytes were analyzed with differential pulse polarography.⁷ To estimate the dissolved Mn^{2+} contents in aqueous electrolytes, 13 mg of spinel powder was dispersed in a 200 ml aqueous solution and stirred for 80 min. The solution pH was controlled by mixing proper amounts of LiClO_4 and HClO_4 .

Electrochemical experiments were performed with an EG&G PARC M362 scanning potentiostat/galvanostat. The proton concentrations in the electrolytes were assessed with a proton-selective glass membrane electrode (DMS digital pH/ion meter, DP-880M). The cell fabrication and

all measurements were carried out at $25 \pm 1^\circ\text{C}$ in a dry box filled with argon.

Results and Discussion

Solvent oxidation, spinel dissolution, and cathodic capacity losses.—As reported previously,⁷ solvent oxidation in 4 V $\text{Li/Li}_x\text{Mn}_2\text{O}_4$ cells takes place on the carbon surface when the composite cathodes are charged at $>4.2 \text{ V}$ (*vs.* Li/Li^+). Figure 1 shows the linear sweep voltammograms traced with a carbon composite electrode (Ketjenblack EC:Teflon binder, 86:14 in weight ratio) in four different solvent mixtures (1:1 vol. ratio) into which 1 M LiClO_4 was dissolved. As demonstrated, the oxidation currents at $>4.0 \text{ V}$ vary significantly according to the nature of the solvents employed: the ethers (tetrahydrofuran and dimethoxyethane) are readily oxidized while the carbonates (propylene carbonate, ethylene carbonate, and diethylcarbonate) are relatively inert. Of the two ethers examined in this study, THF is more oxidizable than DME.

The same electrolyte solutions were loaded in 4 V $\text{Li/Li}_x\text{Mn}_2\text{O}_4$ cells and dissolved Mn^{2+} contents in the intermittently sampled electrolytes were analyzed by differential pulse polarography (Fig. 2). As shown, the spinel dissolution is much more facile in ethers than in carbonates. Also, the dissolved manganese concentration is nearly proportional to the solvent oxidation current shown in Fig. 1. The discharge capacities of $\text{Li/Li}_x\text{Mn}_2\text{O}_4$ cells were traced in the same electrolyte solutions (Fig. 3). Consistently, spinels lose their capacities at faster rates in ethers, and the capacity-loss rate is slower in the carbonate-containing electrolytes. It is evident from the results presented so far that there is a good correlation between the extent of solvent oxidation, spinel dissolution, and capacity losses in spinel electrodes.

Acid generation via solvent oxidation.—As presented in the previous section, among the electrolytes tested in this work, the PC/THF mixture containing 1 M LiClO_4 is most vulnerable to electrochemical oxidation. The solvent oxidation mechanism and oxidation products that are suspected to be involved in the spinel dissolution reaction were examined with this electrolyte system. An inspection of the literature²¹⁻²⁶ reveals that the following oxidation schemes are seemingly pertinent in the $\text{LiClO}_4/\text{THF}$ electrolyte.

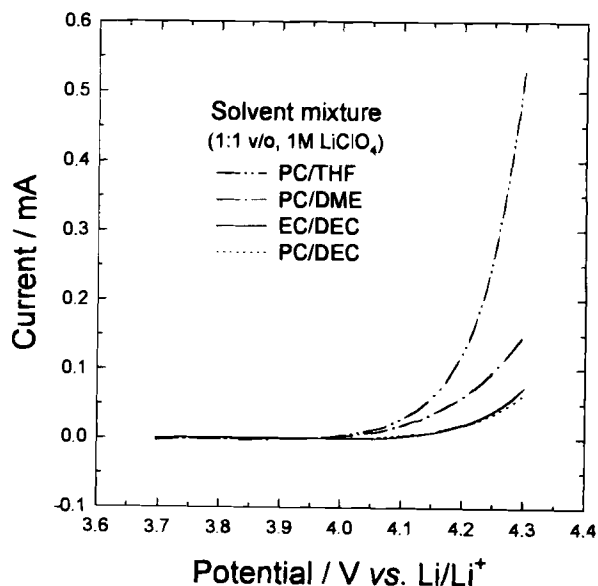


Fig. 1. Linear sweep voltammograms recorded with a composite carbon electrode (Ketjenblack EC:Teflon binder = 86:14 in wt. ratio, apparent area = 1 cm^2) in different mixed solvents (1 : 1 volume ratio with 1 M LiClO_4). Charging current was subtracted from the raw data. Scan rate = 1 mV s^{-1} .

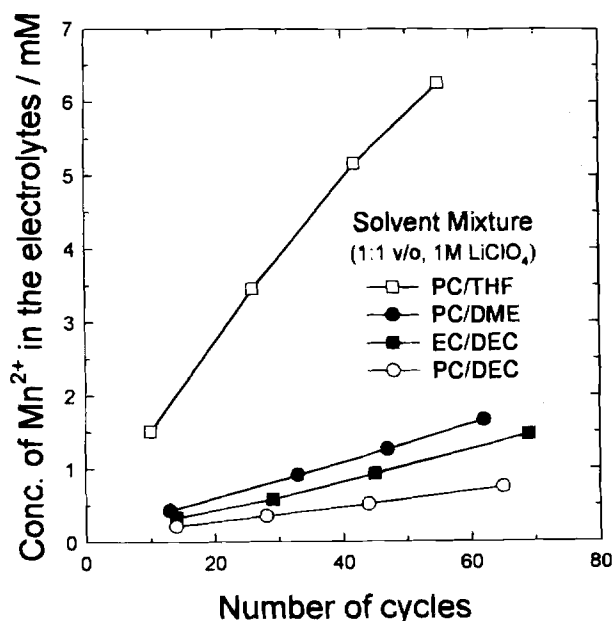
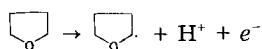
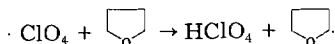
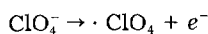


Fig. 2. Mn^{2+} contents dissolved from composite cathodes during charge/discharge cycling. Cycle test was carried out galvanostatically at a current density of 1 mA cm^{-2} at 4.3 to 3.6 V (vs. Li/Li^+). The composite cathodes were prepared with spinel oxides, Ketjenblack EC and Teflon binder (72:20:8 wt ratio). The indicated mixed solvents with 1 M LiClO_4 were used as the electrolyte.

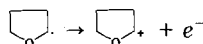
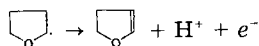
1. Direct oxidation of THF



2. Mediated oxidation via perchlorate radicals



3. Further oxidation



The above schemes illustrate that two different solvent oxidation pathways are possible in the present system: (i) a direct electrochemical oxidation of THF and (ii) a mediated oxidation via perchlorate radicals produced after ClO_4^- oxidation. Some reports²² favor the direct THF oxidation path, whereas the other electron spin resonance (ESR) studies²⁶ support the mediated route by probing radical species in the oxidized media. No matter how the solvent molecules are electrochemically oxidized, the following features are commonly accepted in the literature: (i) oxidation takes place at the α -position of THF molecules and (ii) protons are produced as a result of THF oxidation. Since the early 1980s, electrogenerated acids (EGA) have been widely utilized in a variety of acid-catalyzed electrochemical syntheses in aprotic solvents.²⁴ As a matter of fact, THF has been commonly utilized as an EGA reagent since it is readily oxidized so as to produce protons. In general, ethers are oxidized at the α -position due to the resonance effects whereas the same sites in carbonates are relatively inert due to the electron-withdrawing carbonyl groups (inductive effects). The higher oxidation current peak observed with the DME-containing electrolyte in Fig. 1, in contrast to the carbonates, can thus be explained with the same reasoning.

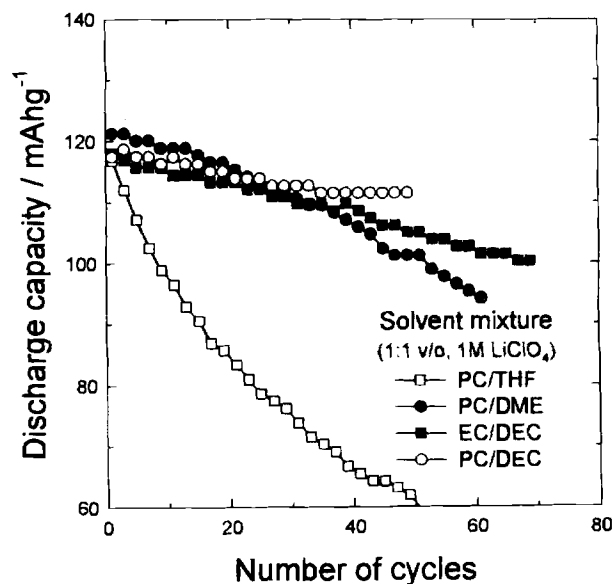


Fig. 3. Discharge capacity profiles of 4 V $Li/Li_xMn_2O_4$ cells in different electrolyte solutions. The cells were designed to be cathode-limited such that the observed discharge capacities represent those of spinels.

The above schemes, suggesting a buildup of protons in oxidized electrolyte solutions, were confirmed by measuring acid concentrations using a proton-selective glass membrane electrode. Figure 4 shows the potential of the glass membrane electrode monitored in four different electrolytes in which a carbon composite electrode was immersed and polarized at 4.2 V to facilitate acid generation. In this figure, a more positive electrode potential reflects a higher proton concentration. As can be seen in Fig. 4, the potential increment in ethers is larger than in carbonates, supporting the postulate that greater amounts of protons are generated when ether-containing electrolytes are electrochemically oxidized.

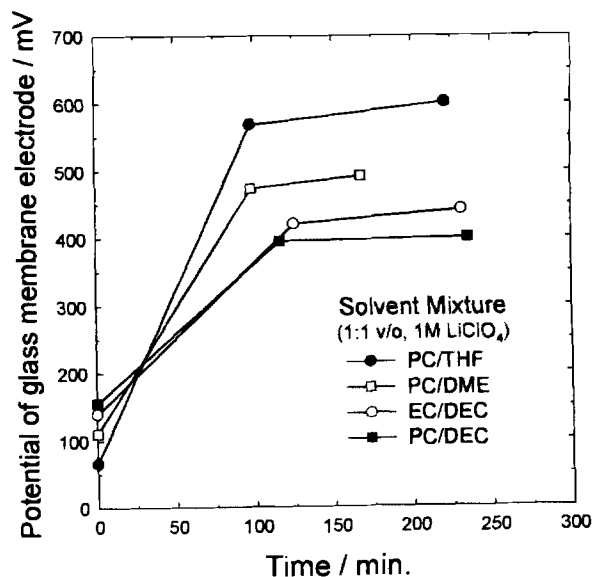


Fig. 4. Potential evolution of a proton-selective glass membrane electrode in different electrolyte solutions. Potential was monitored while a separate composite carbon electrode (Ketjenblack EC : Teflon binder = 86:14 in wt. ratio) was held at 4.2 V (vs. Li/Li^+) to facilitate acid generation. A more positive potential in the scale corresponds to a higher proton concentration.

It is now appropriate to provide additional evidence that acids indeed promote spinel dissolution. It is known that spinel manganese oxides are dissolved in aqueous acid solutions.²⁷ To confirm this, we analyzed Mn^{2+} contents after spinel powders were dispersed and agitated in aqueous acid solutions of different pH. Figure 5 shows the relationship between solution pH and dissolved Mn^{2+} concentrations. Clearly, spinel dissolution is pH-dependent, suggesting that acids play an important role in this reaction.

Dissolution mechanism of $\text{Li}_x\text{Mn}_2\text{O}_4$.—The acid attack on spinel oxides causes a change in their chemical compositions. The weight percent (w/o) of individual element and average Mn valence are listed in Table I, for which the results were obtained with acid-treated spinel powders. For this experiment, spinel powders and a carbon composite electrode were placed closely together in an electrolyte solution while the carbon electrode was polarized at 4.2 V to produce acids. It is presupposed in this experiment that acids are generated at the carbon electrode and then migrate to attack the spinel oxides. After a certain period of time, the spinel powders were collected and their chemical compositions were analyzed. As can be seen in Table I and Fig. 6a, the fractional Li contents steadily decrease with an acid treatment while the Mn fraction initially declines in the earlier stage but then rises gradually. The trace of average Mn valence (Fig. 6b) shows an initial rise but a steady decrease thereafter. The average Mn oxidation state can also be estimated by measuring open-circuit potentials of spinel-loaded composite cathodes. In this experiment, the open-circuit potential (*vs.* Li/Li^+ reference electrode) of a spinel-loaded composite cathode was monitored with a closely spaced carbon electrode being polarized at 4.2 V. As displayed in Fig. 6b, two sets of Mn valence data, one obtained from the chemical analyses and the other from the open-circuit potential measurements, show a similar increasing/decreasing pattern. This time-dependent feature in the chemical composition and Mn oxidation state manifests itself in that the earlier stage Li and Mn extraction is dominant while the oxide framework is relatively intact, leading to an increase in average Mn valence. However, the steady decrease in Mn oxidation state (Fig. 6b) along with a concomitant decrease in oxygen contents (Table I), which is evident at the later stage of acid attack, leads us to infer that oxygen losses from the

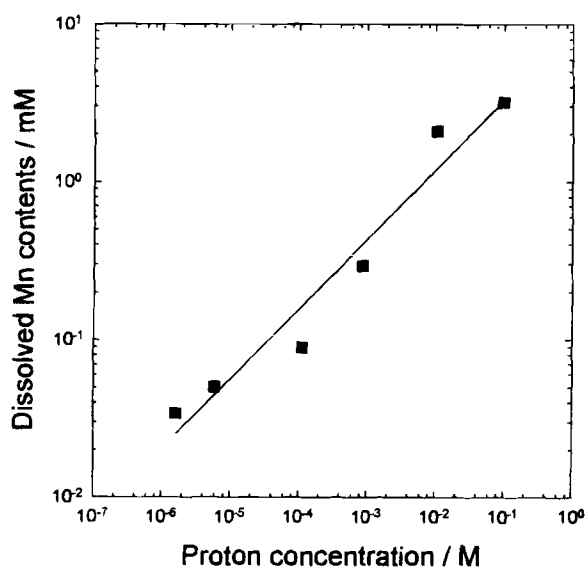


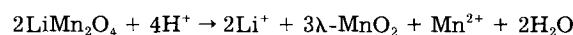
Fig. 5. Dissolved Mn^{2+} contents in aqueous solutions of different pH. For this measurement, 13 mg of spinel powder was dispersed in 200 ml of pH adjusted aqueous solutions and then stirred for 80 min. The solution pH was adjusted by dissolving an appropriate amount of LiClO_4 and HClO_4 in distilled water.

Table I. Analytical data for acid-treated spinel powders.

Exposure time (h)	Li (w/o)	Mn (w/o)	O (w/o)	Z_{Mn}	Empirical formula
0	3.74	59.0	37.26	3.60	$\text{Li}_{0.98}\text{Mn}_{1.95}\text{O}_4$
6.7	3.66	58.3	38.04	3.62	$\text{Li}_{0.97}\text{Mn}_{1.94}\text{O}_4$
30	3.71	59.8	36.43	3.57	$\text{Li}_{0.97}\text{Mn}_{1.97}\text{O}_4$
76.7	3.58	61.0	35.42	3.55	$\text{Li}_{0.93}\text{Mn}_{1.99}\text{O}_4$
Stoichiometric spinel	3.84	60.8	35.36	3.50	$\text{Li}_{1.0}\text{Mn}_{2.0}\text{O}_4$

lattice become more crucial at this stage. The Li and/or Mn-deficient spinels are so thermodynamically stable that their presence is well documented in the literature.^{9,13} Thus, it is not unreasonable to suggest the formation of Li or Mn deficient spinels at the earlier stage. But it is very likely that if the Li or Mn-deficiency exceeds a certain limit, the structural integrity becomes difficult to maintain such that oxide ions are also depleted from the lattice.

Acid-induced spinel dissolution in aqueous solutions has been studied by Hunter.²⁷ He proposed that acids dissolve spinels to produce $\lambda\text{-MnO}_2$ according to the following reaction



Concerning the Mn^{2+} and $\lambda\text{-MnO}_2$ formation, he proposed a disproportionation reaction; $2\text{Mn}^{3+} \rightarrow \text{Mn}^{2+} + \text{Mn}^{4+}$. This dissolution mode implicitly suggests that the relative dissolution rate between the elements (Li:Mn:O) is 2:1:2 and furthermore the relative rate is preserved until the transformation to $\lambda\text{-MnO}_2$ is complete. The results obtained in this study, an earlier stage Li/Mn extraction and oxygen depletion thereafter instead of a steady dissolution of the three elements, however, suggest a different dissolution pathway. The results reported in the previous paper⁷ also indicate that spinels are dissolved even at their charged state as well as at their discharged state. Note that the Mn^{3+} fractions are minimal in the charged spinels (close to

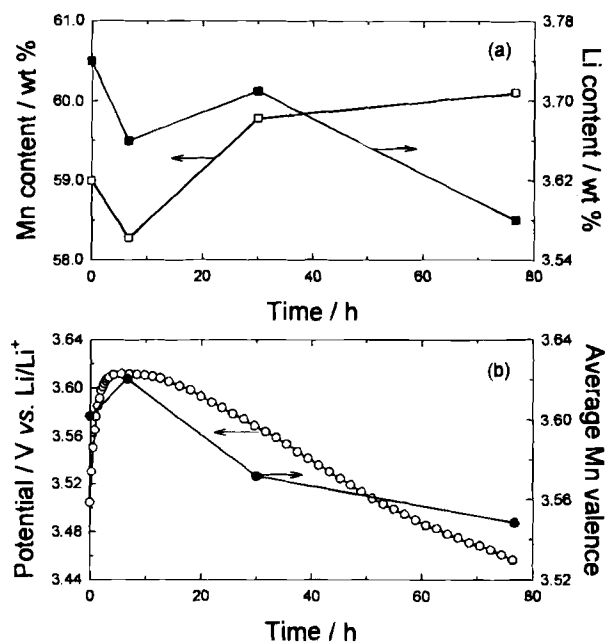


Fig. 6. (a) Fractional Li and Mn contents in acid-attacked spinel powders as a function of treatment time and (b) average Mn valence calculated from the chemical analysis data and open-circuit potential of a composite electrode (spinel:Ketjenblack EC:Teflon binder = 72:20:8 wt. ratio). The electrode potential was monitored while a separate composite carbon electrode (Ketjenblack EC:Teflon binder = 86:14 wt. ratio) was held at 4.2 V (*vs.* Li/Li^+) to facilitate acid generation.

λ - MnO_2) whereas they are maximized at the discharged state (close to the regular spinel). The substantial Mn dissolution from the charged spinels suggests that more tenable dissolution modes than the disproportionation reaction may be involved in the present cell system. At present, it is not clear whether the disproportionation reaction is solely responsible for the dissolution or any other dissolution modes are present. Nevertheless, it would be valuable to point out that the electrolytes used in this study are aprotic in nature in contrast to the aqueous solution in Hunter's work. Along this line, a formation of radical species as proposed in the previous section and their participation in spinel dissolution may provide an additional insight into this issue.

Even if our dissolution mechanism somewhat differs from Hunter's, there appears at least one agreement between the two whereby the three elements (Li, Mn, and oxygen) are depleted from the lattice by acid attack. In a spinel-loaded composite cathode, spinel particles intimately contact with neighboring carbon particles. Under this circumstance, if spinel particles lose Li, Mn, and oxide ions presumably at the outermost surface region, the number of contact points made with carbon particles would be diminished. If this unfavorable situation truly develops along with spinel dissolution, the contact resistance at the spinel/carbon interface as well as the electrode reaction resistance would increase. Then, the composite cathodes cannot be fully charged/discharged due to cell polarizations, leading to capacity losses.

In the meantime, Dahn *et al.*¹⁴ ascribed the spinel capacity losses to a progressive oxygen depletion from the spinel lattice. They proposed the formation of oxygen-deficient spinels ($\text{Li}_x\text{Mn}_2\text{O}_{4-\delta}$, where δ is positive) that discharge at 3.3 V (*vs.* Li/Li^+). In this study, however, all of the acid-treated spinels show an oxygen overstoichiometry (see Table I). Consistently, we could not observe the 3.3 V discharge peak in any spinels.

Lithium salt effects on spinel dissolution.—The electrochemical solvent oxidation and spinel dissolution are also critically dependent on the nature of lithium salts added. For instance, as shown in Fig. 7, proton generation in PC/DME electrolytes is salt-dependent where five different lithium salts were added. It is of value to note two features apparent in Fig. 7. First, the observed initial electrode potentials ($t = 0$) are somewhat different between one solution and another. The initial potential does not

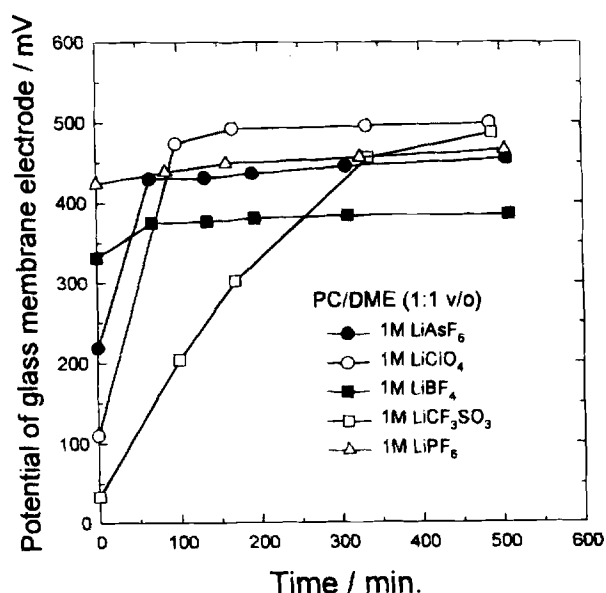
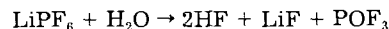


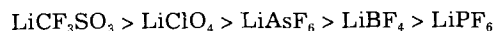
Fig. 7. Potential variations of a proton-selective glass membrane electrode in different salt solutions (PC/DME). The experimental conditions were the same as for Fig. 4.

account for the solvent-derived acids because the composite carbon electrode was not yet polarized. Rather, it reflects the proton concentration in freshly prepared electrolyte solutions. The initial potential values indicate that the fresh solutions made with anions such as PF_6^- , BF_4^- , and AsF_6^- contain a larger amount of protons. This can be ascribed to the impurity water contained in the salts and/or solvents from the known fact that LiPF_6 reacts with traces of water to produce acids (HF) according to the following reaction¹⁰



In order to ascertain the presence of acids in fresh electrolyte solutions, spinel powders were contacted with them, then after a certain period of time, dissolved Mn^{2+} contents were analyzed. As shown in Table II, spinel dissolution is notably high in LiPF_6 - and LiBF_4 -containing electrolytes, reflecting that these electrolytes already have appreciable amounts of protons even in their fresh state. The results in Fig. 7 also illustrate that the LiClO_4 - or LiCF_3SO_3 -containing electrolytes have lesser amounts of protons in their fresh state ($t = 0$) which is evidenced by the negligible Mn dissolution (Table II).

Another noticeable feature in Fig. 7 is the extent of potential rise after the onset of solvent oxidation: a 400 to 500 mV potential rise occurs when a PC/DME solution containing LiCF_3SO_3 or LiClO_4 is electrochemically oxidized, in contrast with a 200 mV increase in the case of LiAsF_6 and 50 mV with LiPF_6 or LiBF_4 . In view of the fact that the potential increase reflects the amounts of solvent-derived acids and the latter in turn is a measure of the degree of solvent oxidation, it is evident that the LiCF_3SO_3 electrolyte is most vulnerable to electrochemical oxidation, whereas in the other extreme the LiPF_6 - or LiBF_4 -containing solvent is most inert. The solvent-derived acid formation rate shows the following decreasing order among the salt solutions



This salt-dependent solvent-derived acid generation can be confirmed by measuring the charges passed during electrochemical solvent oxidation in different salt solutions (Fig. 8). As shown, when the carbon electrode is polarized at 4.2 V, the accumulated charge for solvent oxidation is the highest in the LiCF_3SO_3 solution and the lowest in the LiPF_6 -containing solvent mixture. A comparison of the results in Fig. 7 and 8 shows that the same decreasing order prevails between the extent of acid generation and the charge passed for solvent oxidation.

The observed salt-dependence of acid generation rate suggests that the mediated solvent oxidation seems to be deeply involved in these electrolyte systems, particularly in the LiCF_3SO_3 or LiClO_4 electrolytes. The mediated solvent oxidation via perchlorate radicals has already been suggested in the literature.^{24,25} It is unclear, however, whether the triflate anions play the same role or not.

In Fig. 9, the dissolved Mn^{2+} contents which were analyzed in different salt solutions are plotted as a function of

Table II. Dissolved Mn^{2+} contents in freshly prepared electrolyte solutions containing different Li salts.^a

Li salt (1 M in PC/DME)	Dissolved Mn^{2+} contents (mM)
LiPF_6	0.55
LiBF_4	0.03
LiClO_4	Negligible
LiAsF_6	Negligible
LiCF_3SO_3	Negligible

^a For this experiment, Mn^{2+} concentrations were analyzed after the composite cathodes (spinel powder: Ketjenblack EC:Teflon binder = 72:20:8) were placed in contact with fresh electrolyte solutions for 2 days.

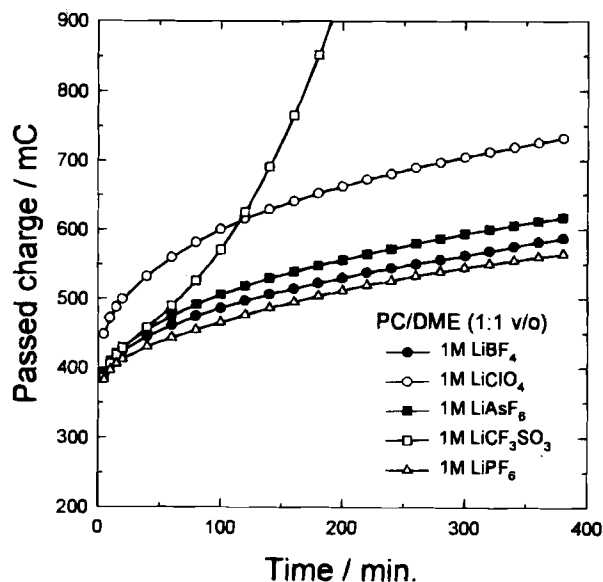


Fig. 8. Accumulated charges passed during solvent oxidation in different salt solutions (PC/DME). The electrode potential was stepped from 3.2 to 4.2 V (vs. Li/Li⁺).

time. As displayed, the extent of spinel dissolution is salt-dependent with the following decreasing order



It has been repeatedly mentioned in this article that spinel dissolution is deeply associated with solvent oxidation and concomitant acid generation. The two listed orders of salt dependence, one the solvent-derived acid generation and the other the extent of spinel dissolution, generally show the same decreasing order. However, there appears a deviation in the LiPF₆-containing electrolyte: The spinel dissolution in this electrolyte is greater than that expected solely from the solvent-derived acid contents. This can surely be explained from the fact that this electrolyte is already contaminated with appreciable amounts of protons in its fresh state due to a reaction with impurity water.

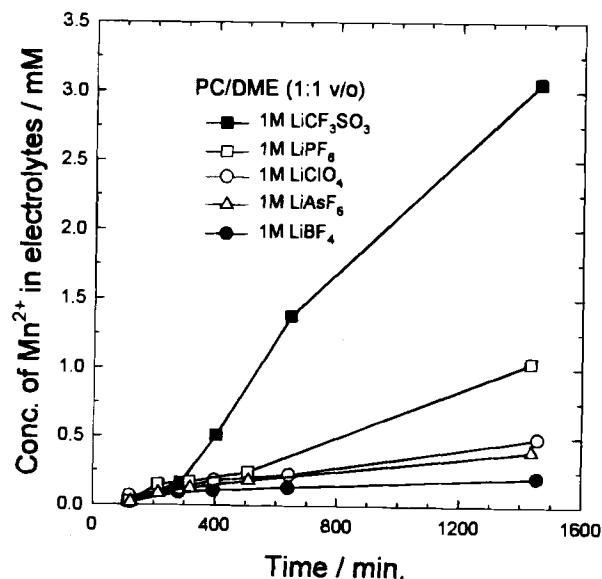


Fig. 9. Dissolved Mn²⁺ contents in different salt solutions (PC/DME) which were monitored while a composite electrode (spinel:Ketjenblack EC:Teflon binder = 72:20:8 wt. ratio) was polarized at 4.2 V (vs. Li/Li⁺).

Conclusions

In this paper, the nature of active species that is responsible for spinel dissolution and the mechanisms for acid generation and spinel dissolution have been elucidated by examining the solvent and salt effects on them. The following points are of value to note.

1. Ethers (THF and DME) are readily oxidized since their α -hydrogens are highly susceptible to oxidation whereas carbonates are relatively inert to this reaction.

2. Protons generated as a result of solvent oxidation play a key role in spinel dissolution. Therefore, spinel dissolution in ethers is more significant as compared to that in carbonates.

3. In the course of acid attack, Li and Mn ions are extracted from the lattice in the initial stage, but in the later stage oxygen loss seems to be dominant. It is believed that the dissolution takes place mainly at the outermost surface region of spinel particles. This would, then, diminish the contact area at the spinel/carbon interface such that cell polarizations become severe due to an increment in the contact resistance and electrode reaction resistance. An ever-increasing cell polarization would make the spinel cathodes not fully charged/discharged, thereby leading to a steady rate of capacity loss.

4. The extent of solvent oxidation and spinel dissolution is also significantly dependent on the nature of salts added. The LiCF₃SO₃ or LiClO₄ electrolytes suffer from severe solvent oxidation such that spinel dissolution is notably high in these electrolytes. Electrolytes containing fluorinated salts are relatively inert to electrochemical oxidation. However, since appreciable amounts of acids are generated by the action of trace water in their fresh state, spinel dissolution in these electrolytes is greater than expected solely from the extent of solvent oxidation.

Acknowledgment

This work has been supported by the Korean Science and Engineering Foundation through the Research Center for Thin Film Fabrication and Crystal Growing of Advanced Materials in Seoul National University

Manuscript submitted Feb 18, 1997; revised manuscript received May 27, 1997.

REFERENCES

- G. Pistoia and G. Wang, *Solid State Ionics*, **66**, 135 (1993).
- L. Chen, X. Huang, E. Kelder, and J. Schoonman, *ibid.*, **76**, 91 (1995).
- H. Huang and P. G. Bruce, *J. Power Sources*, **54**, 52 (1995).
- J. M. Tarascon, E. Wang, F. K. Shokoohi, W. R. McKinnon, and S. Colson, *This Journal*, **138**, 2859 (1991).
- J. M. Tarascon, W. R. McKinnon, F. Coowar, T. N. Bowmer, G. Amatucci, and D. Guyomard, *ibid.*, **141**, 1421 (1994).
- M. M. Thackeray, A. de Kock, M. H. Rossouw, D. Liles, R. Bittihn, and D. Hoge, *ibid.*, **139**, 363 (1992).
- D. H. Jang, Y. J. Shin, and S. M. Oh, *ibid.*, **143**, 2204 (1996).
- A. de Kock, M. H. Rossouw, L. A. de Picciotto, M. M. Thackeray, W. I. F. David, and R. M. Ibberson, *Mater. Res. Bull.*, **25**, 657 (1990).
- M. M. Thackeray, R. J. Gummow, A. de Kock, A. P. de la Harpe, D. C. Liles, and M. H. Rossouw, in *Proceedings of 11th Seminar on Primary and Secondary Battery Technology and Application*, Deerfield Beach, FL, Feb. 1994.
- H. Mao, J. N. Reamers, Q. Jhong, and U. von Sacken, in *Proceedings of the Symposium on Rechargeable Lithium and Lithium Ion Batteries*, S. Megahed, B. M. Barnett, and L. Xie, Editors, PV 94-28, pp. 245-250, The Electrochemical Society Proceeding Series, Pennington, NJ (1995).
- J. M. Tarascon and D. Guyomard, *This Journal*, **138**, 2864 (1991).
- D. Guyomard and J. M. Tarascon, *ibid.*, **139**, 937 (1992).

13. R. J. Gummow, A. de Kock, and M. M. Thackeray, *Solid State Ionics*, **69**, 59 (1994).
14. Y. Gao and J. R. Dahn, *ibid.*, **84**, 33 (1996).
15. J. M. Tarascon, W. R. Mckinnon, F. Coowar, T. N. Bowmer, G. Amatucci, and D. Guyomard, *This Journal*, **141**, 1421 (1994).
16. V. Manev, B. Banov, A. Momchilov, and A. Nassalevska, *J. Power Sources*, **57**, 99 (1995).
17. H.-M. Zhang, Y. Teraoka, and N. Yamazoe, *Chem. Lett.*, 665 (1987).
18. M. S. G. Baythoun and F. R. Sale, *J. Mater. Sci.*, **17**, 2757 (1982).
19. G. H. Jeffery, J. Bassett, J. Mendham, and R. C. Denney, in *Vogel's Textbook of Quantitative Chemical Analysis*, 5th ed., p. 584, Longman Scientific & Technical, New York (1989).
20. A. Wattiaux, J. C. Grenier, M. Pouchard, P. Hagenmuller, *This Journal*, **134**, 1714 (1987).
21. K. Kanamura, S. Toriyama, S. Shiraishi, and Z. Takehara, *ibid.*, **143**, 2548 (1996).
22. A. N. Dey and E. J. Rudd, *ibid.*, **121**, 1294 (1974).
23. F. Ossola, G. Pistoia, R. Seeber, and P. Ugo, *Electrochim. Acta*, **33**, 47 (1988).
24. K. Uneyama, *Top. Curr. Chem.*, **142**, 167 (1987).
25. G. Tourillon, P.-C. Lacaze, and J.-E. Dubois, *J. Electroanal. Chem.*, **100**, 247 (1979).
26. A. H. Maki and D. H. Geske, *J. Chem. Phys.*, **30**, 1356 (1959).
27. J. C. Hunter, *J. Solid State Chem.*, **39**, 142 (1981).

Surface Characterization of Thermally Prepared, Ti-Supported, Ir-Based Electrocatalysts Containing Ti and Sn

T. A. F. Lassali and L. O. S. Bulhões*

Departamento de Química da Universidade Federal de São Carlos/UFSCar, 13565-905, São Carlos, S.P., Brazil

L. M. C. Abeid

Departamento de Química, FFCLRP da Universidade de São Paulo, 14040-901, Ribeirão Preto, S.P., Brazil

J. F. C. Boodts

Departamento de Química, FFCLRP da Universidade de São Paulo, 14040-901, Ribeirão Preto, S.P., Brazil
 Departamento de Química, Universidade Federal de Uberlândia, 38400-902, Uberlândia, M.G., Brazil

ABSTRACT

Surface characterization of Ir-based Ti- and Sn-containing electrodes of nominal composition, $\text{Ir}_{0.3}\text{Ti}_{(0.7-x)}\text{Sn}_x\text{O}_2$ ($0 \leq x \leq 0.7$), was performed *ex situ* by scanning electron microscopy and energy-dispersive x-ray and *in situ* by open-circuit potential measurements and cyclic voltammetry. Despite the use of SnCl_4 as precursor, energy-dispersive x-ray results showed the real composition to be very distinct from nominal due to SnCl_4 volatilization during the calcination step in the electrode preparation procedure. SnCl_4 formation in the precursor mixture was confirmed by visible spectrophotometric measurements. The substitution of TiO_2 by SnO_2 results in a significant increase in electrochemically active surface area, as supported by scanning electron microscopy, anodic voltammetric charge, q_a , and the double-layer capacity, C_{dl} , as a function of composition. Roughness factors between 3600 and 5100 were obtained. A linear C_{dl} vs. q_a graph with an angular coefficient close to one was obtained.

Introduction

Few electrode materials can withstand such adverse conditions as high anodic potentials combined with aggressive chemical conditions (e.g., elevated acidity of medium, chlorine, etc). Among these materials are thermally prepared conductive metallic oxide electrodes, known as dimensionally stable anodes, DSA[®], whose excellent catalytic, mechanical, and corrosion-resistant properties have led to a wealth of important technological applications in different fields.^{1,2} While electrode materials for the chlorine evolution reaction (ClER) have achieved reasonably satisfactory performance, materials aiming at applications involving the oxygen evolution reaction (OER) from strongly acidic solutions can still be improved, especially with respect to their corrosion resistance, i.e., long-term performance.³ A possible way to improve performance is to modify the more usual catalysts (RuO_2 , IrO_2 , etc.) using binary, ternary oxide, or even more complex mixtures in order to modulate the electrocatalytic properties and corrosion resistance. The effect of composition on the electrocatalytic activity of the ternary oxide $\text{Ru}_{0.3}\text{Ti}_{(0.7-x)}\text{Sn}_x\text{O}_2$ from acidic solution was investigated by Boodts and Trasatti.⁴ Later, Onuchukwu and Trasatti investigated the influence of precursor and solvent used

(organic) on the system parameters.⁵ Despite its higher cost, IrO_2 has the advantage over RuO_2 of better resistance to corrosion, while showing only slightly less catalytic activity when compared to the latter.^{6,7} SnO_2 is an interesting candidate as a modulator, since it reduces the catalytic activity of RuO_2 less than TiO_2 .⁴ One problem with SnO_2 is the low yield obtained when common precursor salts are used due to SnCl_4 volatilization.⁸ During a systematic surface characterization study of the $\text{IrO}_2 + \text{SnO}_2$ system, De Pauli and Trasatti⁹ did not encounter SnO_2 yield problems, in apparent contradiction with Comninellis and Vercesi.⁸

In a search for improved electrode materials for the OER from strongly acidic solution, we thought it worthwhile to execute a systematic investigation of the IrO_2 - TiO_2 - SnO_2 system, giving special attention to the SnO_2 yield problem.

Experimental

Electrodes.—A series of eight electrodes, in duplicate, of nominal composition $\text{Ir}_{0.3}\text{Ti}_{(0.7-x)}\text{Sn}_x\text{O}_2$ was prepared, keeping the catalyst loading (IrO_2) constant at 30 mole percent (m/o) while replacing TiO_2 by SnO_2 in 10 m/o steps. Oxide layers were prepared by thermal decomposition at 400°C of the appropriate mixtures of the precursor solutions using TiCl_4 (Aldrich), $\text{IrCl}_3 \cdot x\text{HCl} \cdot y\text{H}_2\text{O}$ (Aldrich), and $\text{SnCl}_4 \cdot 2\text{H}_2\text{O}$ (Vetec) dissolved in HCl 1:1 (v/v) to prevent hydrolysis. In the case of $\text{IrCl}_3 \cdot x\text{HCl} \cdot y\text{H}_2\text{O}$, a few drops of 30% H_2O_2 together with mild heating (~80 to 90°C) were

* Electrochemical Society Active Member.